Regionalization of rainfall thresholds: an aid to landslide hazard evaluation

Giovanni Crosta

Abstract Rainfall, soil properties, and morphology are major factors controlling shallow landsliding. A series of meteorological events that triggered soil slips in northern Italy were studied to define rainfall thresholds and to evaluate a possible regionalization. Soil properties, triggering rainfall, and local lithological and morphometrical settings of different sites were used as input to an infiltration model. The approach allows the recognition of several triggering conditions in the Piedmont, Pre-Alpine and Alpine regions. This suggests the need for different rainfall thresholds with respect to those derived with other methods. Intensity versus rainfall duration relationships become particularly important when related to soil permeability and thickness, and demonstrate the role of antecedent precipitation. Events with exceptional water discharge from obstructed road culverts reveal the role played by anthropic structures in triggering such phenomena. Different approaches to slope stability analysis are shown, taking into account bedrock lithology, topography, seepage, and local saturation conditions.

Key words Soil slips · Rainfall · Threshold · Alps · Slope stability

Introduction

Soil slips are among the most abundant of shallow landslides. In spite of their limited size, soil slips are highly dangerous. Indeed, they exhibit both a high temporal and spatial frequency of occurrence and evolve rapidly into a slurry or debris flow. Their high areal density and small volumes associated with rapid transport and the fact that they often traverse medium gradient terrain make these failures highly hazardous. Consequently, these slope failures have attracted the attention of researchers in mountainous and hilly terrain. Shallow slope failures are also a major concern to planners, because of their ability to cause casualties and of their connection to poorly designed or maintained anthropic structures.

Soil slip/debris flows occur during rainstorms of high intensity and short duration or less frequently, during events of prolonged but relatively moderate intensity, which may be controlled by the antecedent precipitation regime (Campbell 1974; Moser and Hohensinn 1983; Cancelli and Nova 1985; Ellen and Wieczorek 1988; Crosta and others 1990; Buchanan and Savigny 1990). Rainfall thresholds can be defined on an empirical (Caine 1980; Cancelli and Nova 1985) or physical basis. In particular, the latter can take into account specific site conditions by linking regional and local rainfalls to slope and soil characteristics typical of a specific region. Each physiographic area is subject to a particular rainfall regime, with typical rainfall intensity, duration, pattern, etc. Additionally, slope morphometry and soil characteristics vary locally with lithology, morphology, climate and geological history. Mechanical (Moser and Hohensinn 1983; Crosta 1994), hydraulic and physical properties of soils (Pierson 1983; Cancelli and Nova 1985; Crosta 1994; Pradel and Raad 1993; Wilson and Wieczorek 1995), soil thickness, vegetation cover and its contribution to soil strength (Buchanan and Savigny 1990), and local seepage conditions (Iverson 1991; Iverson and Major 1986; Iverson and Reid 1992) are peculiar to a geographical site and may induce variable instability conditions in response to rainfall. It is therefore important to assess the hydrological response of a slope by adopting models able to forecast debris flow initiation by regionalizing rainfall thresholds from site-specific data to help in warning and landslide hazard assessment. From data in the literature and from new investigations, the spatial variability of rainfall conditions generating shallow failures was recognized, together with the need to improve the methods usually applied for shallow slope-stability analysis.

Shallow landslides events

Geomorphological and geological settings

A major problem in landslide hazard assessment involves where and when slope failures will occur. For soil slips

Received: 23 October 1997 · Accepted: 25 June 1997

G. Crosta
Dip. Scienze della Terra, Univ. Studi di Milano, via Mangiagalli 34, I-20133 Milano, Italy

the definition of the time and exact location of failure are particularly troublesome. Soil slips are reported in many different physiographic environments, with different climate, soil, rock, and vegetation types. As a general statement, we can say that rainfall-triggered soil slips occur where soil covered slopes, mostly in non-frictional materials, are sloping at an angle greater than 25°, up to 40°. This definition and the frequency of occurrence of such a combination in Alpine and pre-Alpine landscapes demonstrates the difficulty in identifying particularly hazardous slope areas. Soil slips (soil slip/debris flow, debris flow and debris avalanche, Crosta and others 1990) were investigated in the Alps (Valtellina – Cancelli and Nova 1985; Crosta 1990; Polloni and others 1992; Ossola Valley – Anselmo 1980; Dolomites, Swiss and Austrian Alps – Moser and Hohensinn 1983; Piemonte – Polloni and others 1996 - Valsesia), in the pre-Alps (Southern Alps, Camonica and Brembana Valleys – Baldi and others 1990), in the piedmont areas (Olona valley – Crosta and Marchetti 1993) and at the boundary between the Ligurian Alps and the Northern Apennines (Varenna Valley) (Fig. 1).

This paper presents and discusses the events which have occurred in the last 15 years in Valtellina (1983, 1987), the Camonica and Brembana Valleys (1987), Valsesia (1994), the Olona Valley (1992, 1993) and the Varenna Valley (1993; northern Italy, Fig. 1). Discussion of these events, typical of northern Italy, is fundamental to development of a reliable method for regional rainfall threshold evaluation. The study areas are aligned from north to south, from the Central Alps, where metamorphic and igneous rocks crop out (sub-Alpine crystalline basement, gneiss, paragneiss, micaschist and phyllites; granodioritic and tonalitic intrusions, etc.), to the Pre-Alps (Triassic to Cretaceous Alpine sedimentary rocks including limestone, dolomite, shale, etc.), through the Po Plain made up of fluvioglacial deposits (mostly Oligocene to Miocene sands and gravel), to the Langhe area and up to the Ligurian coast where metamorphic and carbonate rocks crop out. From a geomorphological point of view, Valtellina, forming the upper catchment of the Adda River, has a characteristic U-shaped valley profile, with hanging tributary valleys and very steep slopes (maximum elevations 4000 m) in metamorphic rocks, covered by colluvial and glacial deposits. The Camonica and Brembana Valleys, catchments of the Oglio and Brembo Rivers, respectively, exhibit a similar morphology, with lower maximum elevations of up to 2500 m and dominant sedimentary bedrock formations. The upper Olona Valley, in the Piedmont region, is characterized by a very steep and narrow incision through glacial and fluvioglacial deposits with rare flyschoid soft rock outcrops and a maximum elevation of 500 m in the upper catchment areas. The Sesia Valley is a U-shaped glacial valley underlaid by igneous and metamorphic rocks, covered by glacial deposits and with maximum elevations over 4000 m. On the opposite side of the Po Plain, the Langhe area is characterized by rounded hills with relatively low-gradient terrain controlled by northward-dipping strata of flyschoid weak marl and sandstone rocks. The Varenna catchment is an example of the steep morphology peculiar to all the Ligurian river basins (elevations ranging from 0 to 950 masl)

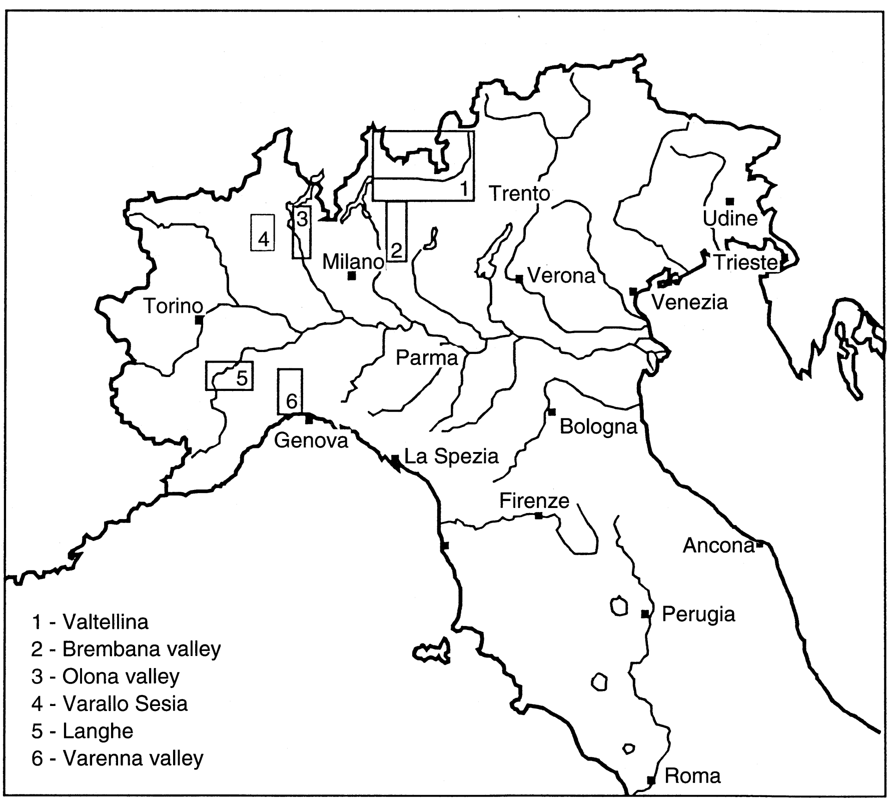

Fig. 1
Location of the six areas investigated in northern Italy

with it being intensely vegetated and relatively short. All the areas exhibit moderate to high urbanization, which is the main cause of human casualties and economic losses due to shallow failures.

Rainfall conditions triggering soil slips

The 1983 and 1987 Alpine and pre-Alpine events

Two main rainfall events have triggered abundant shallow landslides in the last two decades, within the Alpine and pre-Alpine regions. These took place in May 1983 and July 1987, in Valtellina. The first event was characterized by heavy antecedent rainfall of 104–289 mm over 30 days, and by prolonged continuous rainfall for a total duration of 10–15 days (193–453 mm). Two successive bursts, occuring on 14–16 May with 78–248 mm and 21–23 May with 53–205 mm total rainfall, had a maximum intensity of 41–108 mm/day (Guzzetti and others 1992). In the upper and middle part of Valtellina (Fig. 1) about 200 soil slips were mapped and described (Polloni and others 1992). As a result of just one of these slope failures 18 people died at Tresenda (Cancelli and Nova 1985).

In July 1987, an exceptional meteoric event was recorded in the Alps. Following a relatively dry summer, between 84 mm and 511 mm of rain fell in a 3-day storm from 17–19 July. Rainfall intensities ranged between 11 mm/h and 47 mm/h, with a maximum of about 170 mm in 7 h (Guzzetti and others 1992). Several hundred soil slips and soil slip/debris flows were recorded almost simultaneously, with a major concentration in the Orobic sector on the southern valley side (Crosta 1990; Crosta and others 1990). The Camonica and Brembana Valleys (Fig. 1) were hit by the same event (Baldi and others 1990) and numerous failures were reported.

The 1994 Piemonte-Langhe event

During November 1994 an exceptional meteoric event occurred in the Piemonte region. Major consequences were recorded in the Langhe area of the southern Piemonte (Polloni and others 1996) while few soil slips occurred to the north in the Sesia Valley (Fig. 1). A single soil slip at Varallo Sesia killed 14 people. In the Langhe area, 263 mm of rain fell in 3 days from 4–6 November, with intensities ranging between 28 and 40 mm/h. Preliminary estimates suggest that the precipitation had a 1000-year return period. The antecedent precipitation amounted to 62 mm (Polloni and others 1996). Thousands of soil slips, with an areal density up to 180 events per km^2 were observed after 124 mm of cummulative rainfall, as recorded at the Alba and Treiso rain gauges (Fig. 2). This was quite similar to the 1972 event which recorded 130 mm with about 50 mm antecedent rainfall, and a little lower than that in 1968 which totalled 195 mm with 28 mm of antecedent rainfall (Polloni and others 1996).

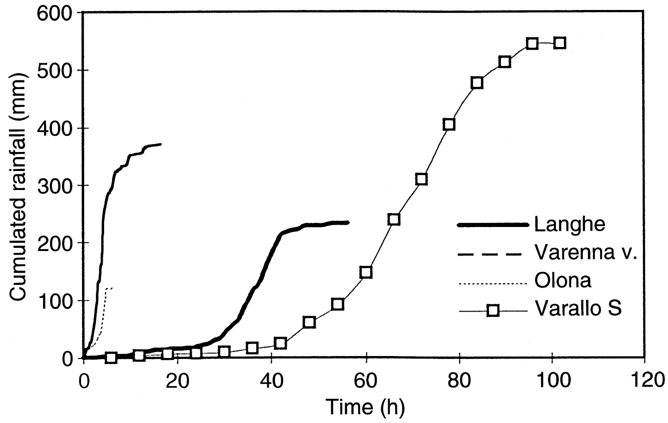

Fig. 2
Cumulative rainfall for some of the events. Rainfall for the two events in Valtellina are not reported because they are spread over a larger time interval (Crosta 1990; Guzzetti and others 1992; Polloni and others 1992)

A few hundred kilometers from the Langhe region, at Varallo Sesia (Fig. 1), a cummulative precipitation of about 560 mm was recorded during 5 days. The peak intensity of about 20 mm/h was maintained for about 20 h, and the cummulative daily precipitation reached 313.2 mm (Fig. 2, return period greater than 100 years). A few soil slips occurred in the Sesia Valley. One of these originated in glacial deposits as a consequence of the natural susceptibility of the terrain to instability (steepness, relatively shallow bedrock surface, bedrock fracture flow from slightly karstic enlarged fractures, etc.) and indirect anthropic action of runoff concentrated on paved roads. In particular, runoff was concentrated because of the malfunction and obstruction of two road culverts, the incorrect design of lateral ditches and interception by a paved road (constructed in the early 1960 s) cutting a few times through the slope and passing just uphill of the soil slip scarp at 570 masl. Fourteen people died and three buildings, dating back to the beginning of the nineteenth century, were destroyed.

The role played by artificial structures was significant in triggering and controlling many of the shallow slope failures, as already demonstrated in some of the more tragic events, such as at Tresenda and Tartano in Valtellina. A detailed analysis of the event has been conducted, taking into account the available rainfall intensity data of the Varallo Sesia rain gauge and the enlargement of the contributing basin, to show the importance of these structures. The Rational Runoff Method (Pilgrim 1986) was adopted to evaluate the increase in water discharge along the paved road (Fig. 3) because of culvert malfunctioning. The paved road and the almost obstructed culverts were allowed to take in a large part of runoff water (see arrows in Fig. 3) fed by 5 secondary catchments for a total surface area of 0.075 km^2. The net increase in water discharge of 0.028 m^3 s^{-1}, in proximity to the soil slip scar, ranged between 2 and 2.5 times the maximum precipitation contribution. This contribution could have been a

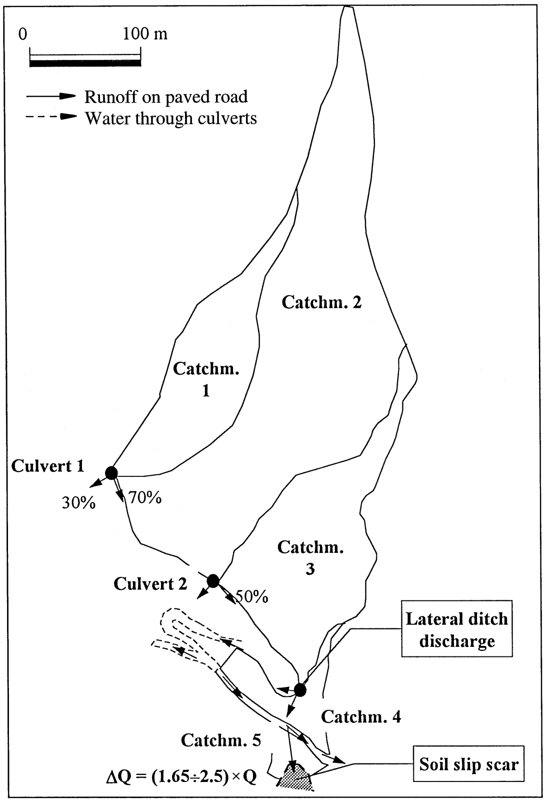

Fig. 3
Sketch showing the area involved in a soil slip failure at Varallo Sesia that caused 14 casualties. Two culverts, one lateral ditch and the paved road functioned as a water collecting system that discharged directly on the soil slip detachment area. Anthropic induced shallow failures are among the more common type of these phenomena. A similar event caused 18 casualties at Tresenda (Valtellina 1983, Cancelli and Nova 1985)

major cause of instability, more than compensating for that intercepted by the dense tree cover.

The Olona valley events

A peculiar event occurred on 1 June 1992 in the Olona Valley (Fig. 1). The event lasted only about 6 h and was characterized by high total precipitation of 125–140 mm, and scarce rainfall of only 119 mm in the preceding 30 days. Rain gauges at Varese, Venegono, and Busto Arsizio in the area recorded peak intensities of 60 mm/h and 123 mm/5h30min. Historical analysis suggests that the recurrence interval of such event ranges between 75 and 100 years. About 100 shallow slope failures (soil slips and soil slip/debris flows) were mapped in a 18 km^2 area embracing the steep valley sides and some of the upper terraces (Crosta and Marchetti 1993).
The following year a heavy storm, preceded by one week's antecedent rainfall of between 160 mm and 284 mm, hit the territory of Varese and the Lake Maggiore. Between 140 mm and 190 mm of rain fell in 1 day, with rainfall intensities between 30 and 65 mm/h. Tens of shallow failures occurred in the area, causing one casualty and a few injuries.

The Ligurian coast

Meteorological conditions change at a local and regional scale, due to localized storm cells or to regional cyclonic conditions. The latter is the case when moving from the Alpine–pre-Alpine sectors to the Thyrrenian coast. Here a persistent cyclonic Thyrrenian circulation is often established which can induce heavy rainstorms along the northeastern coastline of Ligury and Tuscany. At the same time, the close proximity of the drainage divide to the coastline causes major rainstorms to discharge on its southern side, thus controlling some peculiar characteristics of the Ligurian coast basins, such as steepness, frequent slope instability, potential for rapid flooding and sediment yield.
The event of September 1993 in the Varenna Valley, uphill from the town of Genoa, lasted 3 days with the maximum intensity and total precipitation of 450 mm concentrated in a single day (Fig. 1). The closest rain gauge, at Madonna della Guardia on the catchment divide, recorded a maximum hourly intensity of 108 mm. Total cummulative daily precipitation was 363.4 mm, which fell in about 12 hours (Fig. 2). These values are the highest ever recorded in the area. Their exceptional nature is clear if compared with the precipitation during other events (as shown in Fig. 2). In 1994, a second event struck the area with a maximum hourly intensity of 70.2 mm and a peak daily precipitation of 205.2 mm. While the 1993 event induced more than 350 soil slips with a maximum spatial frequency of 107 per km^2, the 1994 event was characterized by few reactivations and almost an absence of soil slips.
A peculiarity of some of the surveyed failures was the presence of old dry stone walls, completely covered by colluviated material, associated with the slide scar. This coincidence could be due to drainage induced by the coarse dry stone wall material, which acts as a conduit to collect seepage and to increase locally the water pressure, thereby decreasing the stability of the soil cover. Again, the presence of artificial structures appears to be one of the factors controlling slope instability.

Slope morphometry and soil properties

Morphometric features and geotechnical soil properties, including physical, mechanical and hydraulic parameters, are the two most important groups of factors controlling the origin and development of soil slips and soil slip/debris flows. Morphometric and soil property data were collected from different Italian sites, allowing the recognition of some important similarities among them and with other phenomena in the literature. These may, in turn, be used to differentiate among groups of events.

Slope morphometry

Soil slips and soil slip/debris flows are reported in a variety of environments. In the study areas they were observed on unchannelled, zero-order basins or slight slope concavities; on channelled slopes of first- or higher-order basins; and on open hillslopes (Crosta and others 1990) or spurs, with single or multiple sources resembling sheet-like or spoon-like scars. Source areas are located in different positions with respect to the main divide. They occur close to the top and near the toe of slopes. Campbell (1974) reported shallow soil slips on natural slopes of 18.4°–45°. In the Alpine and pre-Alpine regions, shallow landslides were mapped on slopes ranging between 25° and 40°, close to the divide, on very steep anthropic benching, and at the foot of the slope. In the piedmont areas, soil slips developed on steep (30°–40°), heavily vegetated slopes. Slopes, ranging between 30 and 60 m in length, are limited at the top by flat areas of glacial and fluvioglacial terraces, and at the bottom by the Holocene deposits of the Olona River. Grass-covered slopes are particularly prone to soil slips with a 0.2–0.3-m average thickness. Frequently, failures occur also on steep forested areas both in the Alpine and piedmont regions. In the Ligurian Alps, soil slips occurred on slopes of 35°–45°,with the eroded soil thickness of 0.3–0.7 m and were more abundant toward the toe of the slopes, in grass-covered terrain.

In all cases, a strong control on soil slips is the presence of a shallow bedrock. Its effect on soil cover thickness along steep slopes or on the establishment of subsurface flow is still to be evaluated. The depth of soil slip scars is influenced by the thickness of the soil cover and commonly ranges between 0.20 and 0.50 m. Locally, scars up to 1.2 m deep were recorded in glacial deposits (Valtellina, Crosta 1990). The downhill evolution of the moving mass seems to be controlled both by morphometrical characteristics of the slope (i.e., open or channelled slopes, channel or slope geometry, etc.) and by soil properties (i.e., relative density, silt-clay content, etc.).

Soil properties

Colluvial, regolithic, glacial and fluvioglacial materials are among the soils involved in soil slips. Their deposits were sampled and a set of tests were performed, including identification (grain size and Atterberg limits), direct and torsional shear tests, triaxial tests, etc., to give a technical and mechanical description of soil types and properties. Grain-size analyses, on samples collected from various sites, provide the distribution of soil types according to the different regions of provenance (Fig. 4). Shear strength properties were found to be typical of sandy soils with a variable percentage of silt and clay. The computed angles of internal friction (ϕ) fit well with sandy soils and can be correlated, when possible, to the Atterberg limits (Table 1). Very low cohesion values were measured in many soils, while a higher in situ cohesion can be induced by the reinforcement of the root system and soil suction produced by negative pore pressure.

Soil permeability was estimated, for unfailed slopes and in the source areas of soil slips, by laboratory tests or by the D_{10} and D_{60} relationships with grain-size distribution (Crosta 1994) and the subdivision proposed by Casagrande and Fadum (1940) of SM: 10^{-3}–10^{-4} cm/s; SC: 10^{-4}–10^{-5} cm/s; GM: 10^{-2}–10^{-3} cm/s; ML: 10^{-4}–10^{-5} cm/s. Indirect estimates of soil permeability compare well with permeability values computed on the basis of in situ measurements using infiltrometers carried out in Valtellina and at Varallo Sesia (Table 1). Porosity and effective porosity were evaluated in different samples, at different moisture contents and at different times of the year, showing large variations. Suction was provisionally estimated by means of empirical relationships proposed by Wallace (1977). In situ measurements are presently obtained by tensiometers. Matrix suction close to the desaturation point can be obtained by empirical relationships with grain-size distribution parameters (D_{10}, D_{60}; $P_{des} = 30/D_{10} \div 60/D_{10}$). Matrix suction close to the resaturation point ranges between 30% and 50% of the estimated desaturation value. The extreme values resulting from the analysis of available data were in the range of 0.3 –6.0 m, expressed as height of the equivalent water column, going from conditions close to resaturation point to those of desaturation. Considering the most dangerous months of the year of May-June, October-November in all the studied areas, for the occurrence of soil slip events, an average value of 0.8–1.0 m can be considered for these materials according to values reported in the literature and in situ measurements. Higher values were obtained for finer, sometimes structured, soils from the

Table 1

Soil properties measured on samples from different sites (γ_n unit weight; *LL* liquid limit; *PL* plastic limit; ϕ friction angle; ϕ_r residual friction angle; *C* cohesion; *k* hydraulic conductivity; <0.074 mm percentage of material finer than 0.074 mm; <2 μm percentage of material finer than 2 μm; *USCS* unified soil classification system)

Locality	γ_n kN/m^3	LL %	PL %	≤0.074 mm %	≤2 μm %	USCS	ϕ °	ϕ_r °	c kN/m^2	k cm/s
Valtellina	18–21	18–32	10–14	5–18	1–11	SM, SC, GP-GM	30–40	17–33	<40	1×10^{-3}–2×10^{-4}
Olona	15–18	31–35	6– 9	17–64	4–7	SM, ML	30–35	–	–	–
Varallo S.	15–18	29–47	22–38	15–36	<10	SC	33–35	28–29	37–75	3×10^{-3}–2×10^{-5}
Varenna	17–20	24–55	21–33	19–83	3–23.5	SC, SM	31.8–36.4	26.5–33.6	–	–
Langhe	18–19	30–45	15–25	12–54	6–31	SC, SM	–	26–31	2–4	–

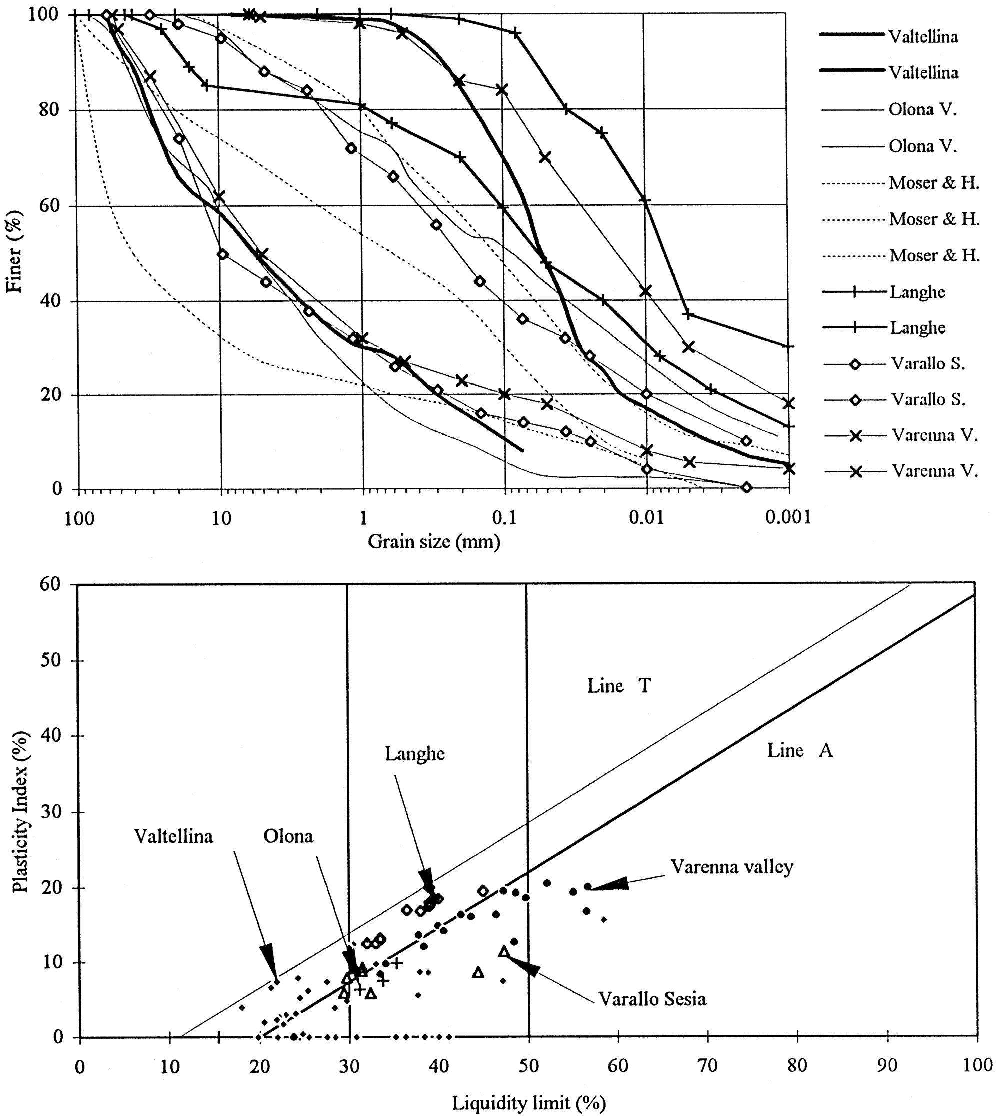

Fig. 4
Grain-size distribution and Casagrande plasticity chart for samples collected from soil slip and soil slip/debris flows source areas (Data reported by Moser and Hohensinn (1983) abbreviated as M. & H. in the legend are also shown)

Olona Valley. Collection of physical, hydraulic and mechanical soil properties has been fundamental to accomplishing a zonation of the territory and whenever possible slope stability analysis was performed to support this zonation.

Slope stability analysis

Two different types of soil-slip scars were recognized in the study areas: sheet- and spoon-shaped; similar to observations reported by Moser and Hohensinn (1983), Buchanan and Savigny (1990), Crosta (1990), Crosta and others (1990), and Anderson and Sitar (1995). Sheet- or spoon-shaped surfaces influence the stability analysis that can be performed. An infinite-slope stability analysis is usually preferred for its simplicity, the ease in introducing different groundwater conditions, and because of the failure geometry with characteristic low values of the depth to length ratio (D/L).

According to the infinite-slope stability model (Skempton and DeLory 1957):

$$Fs = \frac{C'}{\gamma_{\mathrm{sat}} H \cos^2\beta \tan\beta} + \frac{(\gamma_{\mathrm{sat}} - m\,\gamma_{\mathrm{w}})}{\gamma_{\mathrm{sat}}}\,\frac{\tan\phi'}{\tan\beta} \tag{1}$$

The worst stability condition in a soil layer with cohesion (C') and friction (ϕ'), where the water table is at any level mH from the failure surface (Fig. 5), occurs for seepage parallel to the slope (β). More conservative situations, with more hazardous seepage conditions are possible (Iverson 1991; Iverson and Major 1986; Iverson and Reid 1992) in saturated soil layers with a continuous water recharge. Seepage parallel to the slope is acceptable where soil cover is thick, isotropic and homogeneous, over a deep-seated bedrock. This situation occurs where large water recharge areas, such as long hillslopes, are present, or for shallow-lying bedrock with limited recharge areas. Parallel-to-slope seepage can be an unnecessary restriction because small variations in permeability, localized bedrock irregularities or presence of macropores, can induce a nonparallel-to-slope seepage produc-

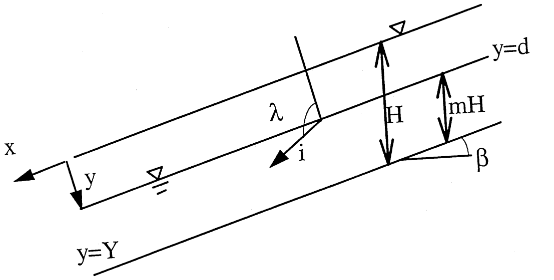

Fig. 5
Sketch representing variables for the general solution of infinite slope stability with variable seepage flow direction (after Iverson 1991)

ing very important and effective deviations for slope stability (Pierson 1983; Iverson 1991; Iverson and Major 1986; Iverson and Reid 1992; Reid and Iverson 1992).
Field observations showed a large number of soil slips on slopes with an average gradient of 30°–35°. Material properties were found by back-calculation to range between 33° and 36° for the friction angle (ϕ) and cohesion (C) between 1 and 3 kPa. These results are in agreement with the laboratory tests.
The relative influence of seepage direction, strength parameters, soil thickness and slope gradient can be evaluated in a deterministic or probabilistic fashion. A sensitivity analysis was performed adopting different approaches to calculate the factor of safety. A saturated slope condition was considered to analyze the influence of seepage flow angle; and a partially saturated slope with a deep water table to analyze changes due to an advancing wetting front. The equation proposed by Iverson (1991) for a more general situation (Fig. 5) was used:

$$Fs = \frac{\tan\phi'}{\tan\beta} + \frac{[(d/Y)-1](\partial p/\partial y)\tan\phi'}{\gamma_{\mathrm{sat}}\sin\beta} + \frac{C'}{\gamma_{\mathrm{sat}}\,Y\sin\beta} \tag{2}$$

where

$$\frac{\partial p}{\partial y} = \gamma_{\mathrm{w}}(i\cos\lambda + \cos\beta) = \gamma_{\mathrm{w}}\left(\frac{\sin\beta}{\tan\lambda} + \cos\beta\right) \tag{3}$$

and ϕ' is the angle of internal friction, C' is the cohesion, d is the water table depth, Y is the depth of the failure plane, β is the slope angle, λ is the seepage flow direction from the outward normal to the slope for an hydraulically isotropic soil, γ_{sat} is the saturated soil unit weight and γ_{w} is the water unit weight, $\partial p/\partial y$ is the mean pore water pressure gradient.
For the case of a completely saturated slope the following equation was used:

$$Fs = \frac{\left[(\gamma'\cos\beta + \gamma_{\mathrm{w}}\sin(\delta-\beta))\tan\phi + \dfrac{C}{H}\right]}{\gamma\sin\beta + \gamma_{\mathrm{w}}\,i\cos(\delta-\beta)} \tag{4}$$

where β is the slope angle, δ is the seepage flow angle (with respect to the horizontal), i is the hydraulic gradient and H is the depth of the failure surface. The factor of safety decreases when considering outward seepage which reaches a critical condition where flow is normal to the slope (Fig. 6). The lowest factor of safety is associated with slope gradient and the shallowest failure surface.
Different opinions exist on how subsurface flow can develop and what kind of mechanism and environmental factors control slope instability. Wilson and Wieczorek (1995) have suggested that precipitation can induce the formation of a saturated zone and the subsequent rising of the water table, especially where shallow bedrock exists (Fig. 7a). A different model (Pradel and Raad 1993; Crosta and Marchetti 1993; Rahardjo and others 1995) suggests that a temporary perched groundwater table forms in thicker soil covers, between the topographic surface and the wetting front (Fig. 7b), reducing the negative pore-water pressure, and starting parallel-to-slope seepage that contributes to slope instability. The last approach must consider the role of matrix suction in increasing the shear strength of soils. It is important to define which distribution was selected to model the component of negative pore pressure (Rahardjo and others 1995) and its changes with depth (Fig. 8). Rahardjo and others (1995) consider the presence of a deep water table, with inclination equal to the slope, $\beta=\delta$, with a negative pore-pressure distribution coupled with an advancing wetting front or with a shallower pore-pressure distribution. Starting from the approach of Rahardjo and others (1995), some analyses were performed to examine the effects of such a situation on the stability of a soil layer with the failure surface at a variable depth. The analyses were based on the following equations proposed by Rahardjo and others (1995), for the hydrostatic condition:

$$Fs = \frac{\tan\phi'}{\tan\beta} + \left(\frac{C'}{\gamma_{\mathrm{sat}}(H_{\mathrm{w}}-z)}\right)\frac{1}{\sin\beta\cos\beta} + \left(\frac{z}{H_{\mathrm{w}}-z}\right)\left(\frac{\gamma_{\mathrm{w}}}{\gamma_{\mathrm{sat}}}\right)\left(\frac{\tan\phi_{\mathrm{b}}}{\tan\beta}\right) \tag{5}$$

for the non-hydrostatic condition:
a) surface saturation:

$$Fs = \frac{\tan\phi'}{\tan\beta} + \left(\frac{C'}{\gamma_{\mathrm{sat}}(H_{\mathrm{w}}-z)}\right)\frac{1}{\sin\beta\cos\beta} + \left(\frac{H_{\mathrm{w}}}{z_{\mathrm{s}}}-1\right)\left(\frac{\gamma_{\mathrm{w}}}{\gamma_{\mathrm{sat}}}\right)\left(\frac{\tan\phi_{\mathrm{b}}}{\tan\beta}\right) \tag{6}$$

b) advancing wetting front:

$$Fs = \frac{\tan\phi'}{\tan\beta} + \left(\frac{C'}{\gamma_{\mathrm{sat}}(H_{\mathrm{w}}-z)}\right)\frac{1}{\sin\beta\cos\beta} \tag{7}$$

c) perched water table:

$$Fs = \frac{\tan\phi'}{\tan\beta} + \left(\frac{C'}{\gamma_{\mathrm{sat}}(H_{\mathrm{w}}-z)}\right)\frac{1}{\sin\beta\cos\beta} - \left(\frac{\gamma_{\mathrm{w}}}{\gamma_{\mathrm{sat}}}\right)\left(\frac{\tan\phi_{\mathrm{b}}}{\tan\beta}\right) \tag{8}$$

where H_w is the depth of the water table, z_s is the depth of the wetting front, z is the distance of the failure sur-

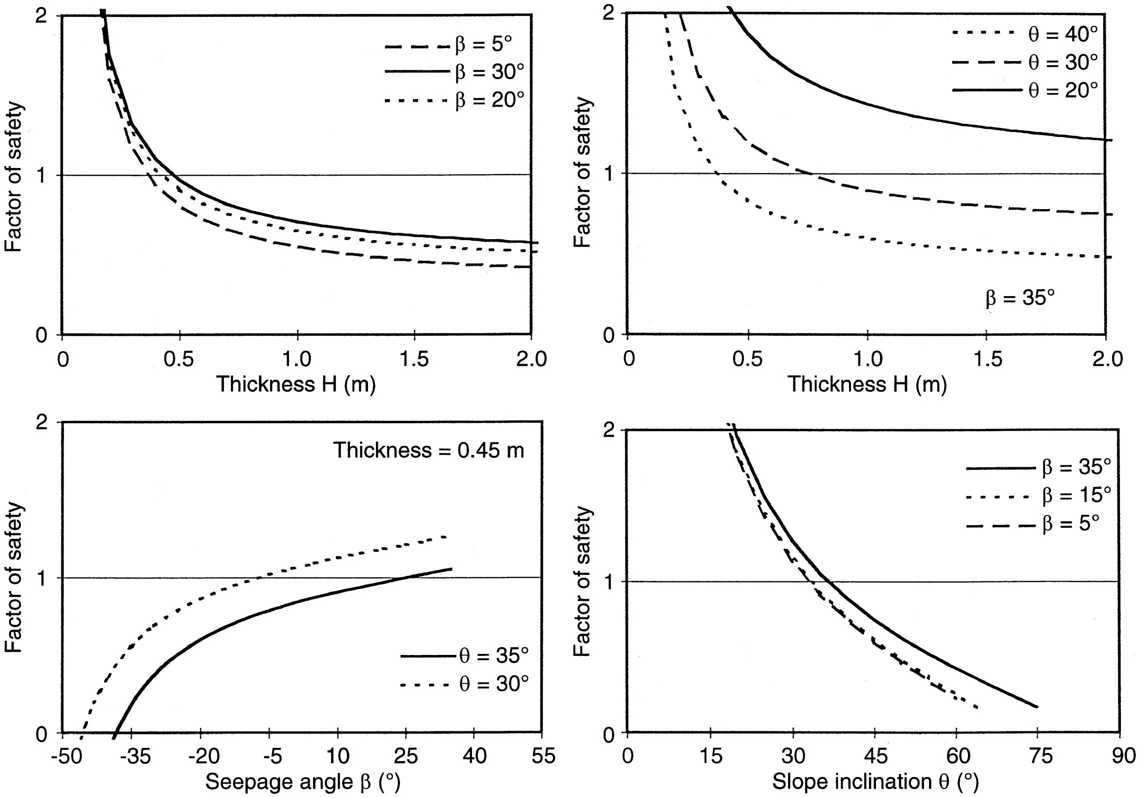

Fig. 6
Results of slope stability analyses in the presence of seepage with different flow directions in a fully saturated slope ($C = 1$ kPa, $\phi = 33°$, H = 0.45 m)

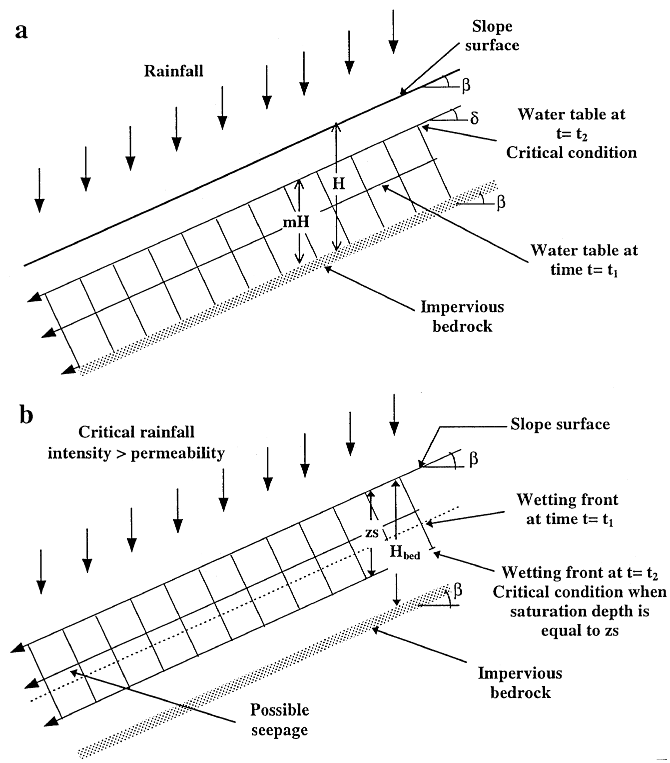

Fig. 7a, b
Two possible mechanisms for the saturation and the instabilization of surficial deposits: **a** rising water table with parallel to slope seepage; **b** wetting front advancing from the slope surface

face from the water table, and ϕ_b is the angle which represents the rate of increase in shear strength relative to matrix suction. In the case of a very deep water table, in soil layers where no negative pore pressure gradient is present or at intermediate depth where the surface water and deep water table influences are negligible, these equations can be modified by considering a constant suction value at the wetting front (case d in Fig. 8) and independent of depth (the adopted subdivision is used through the successive figures).

Results of such analyses are summarized in Fig. 9 which shows a decrease in the factor of safety when moving the surface of failure close to the water table level. This decrease is also observed when passing from the nonhydrostatic condition a to condition c (Eqs. 6–8). The factor of safety decreases rapidly for slip surfaces near to the ground surface. Changes in water moisture are more effective for shallow slope failures, because the factor of safety generally is lower in the wetted zone. One more interesting observation is the dependence of the factor of safety on the wetted depth (z_s) only in case a where saturation takes place only at the topographic surface and negative pore pressures change with depth.

These slope stability approaches are useful in developing soil slip susceptibility and hazard zonation maps. The importance of field data and back calculation becomes evident when looking at the definition of critical thickness and critical saturated thickness. To correlate slope failure to rainfall it is necessary to define the water-table level or the saturated thickness. This correlation allows the definition of the possible time of failure after the onset of precipitation for a given range of rainfall intensities and soil properties. Since rainfall intensity and soil properties are functions of specific physiographical, geological, and morphological environments, this correlation is mandatory for any susceptibility analysis and hazard zonation.

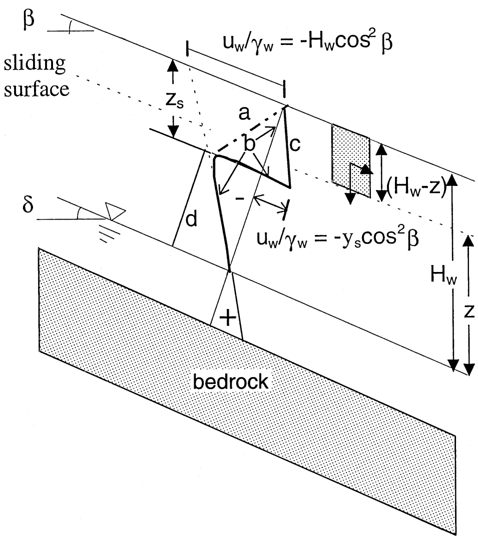

Fig. 8
Sketch representing variables and assumptions (marked as a, b, c) for pore pressure distribution within the soil mass (modified after Rahardjo and others 1995; see text for comments

The role of rainfall and infiltration as controlling and triggering factors

Groundwater conditions in soil-covered hillslopes are controlled by water infiltration from the surface (Buchanan and Savigny 1990). Subsurface flows parallel to the slope originate by the rising of a water table or the development of a perched water table between the surface and an advancing wetting front. This can be a consequence of an increase in moisture content at a specific depth up to saturation. From this point on, a perched water table can develop at a depth, changing with rainfall characteristics,

Fig. 9
Results of sensitivity analyses for shallow slope failures on the basis of different hypotheses: hydrostatic and nonhydrostatic (n.h.), with and without matrix suction. Nonhydrostatic conditions a, b and c are those sketched in Fig. 8 with $\phi=33°$, $\phi_b=26°$, $c=1$ kPa, $\beta=30°$, $P_{suction}=20$ cm

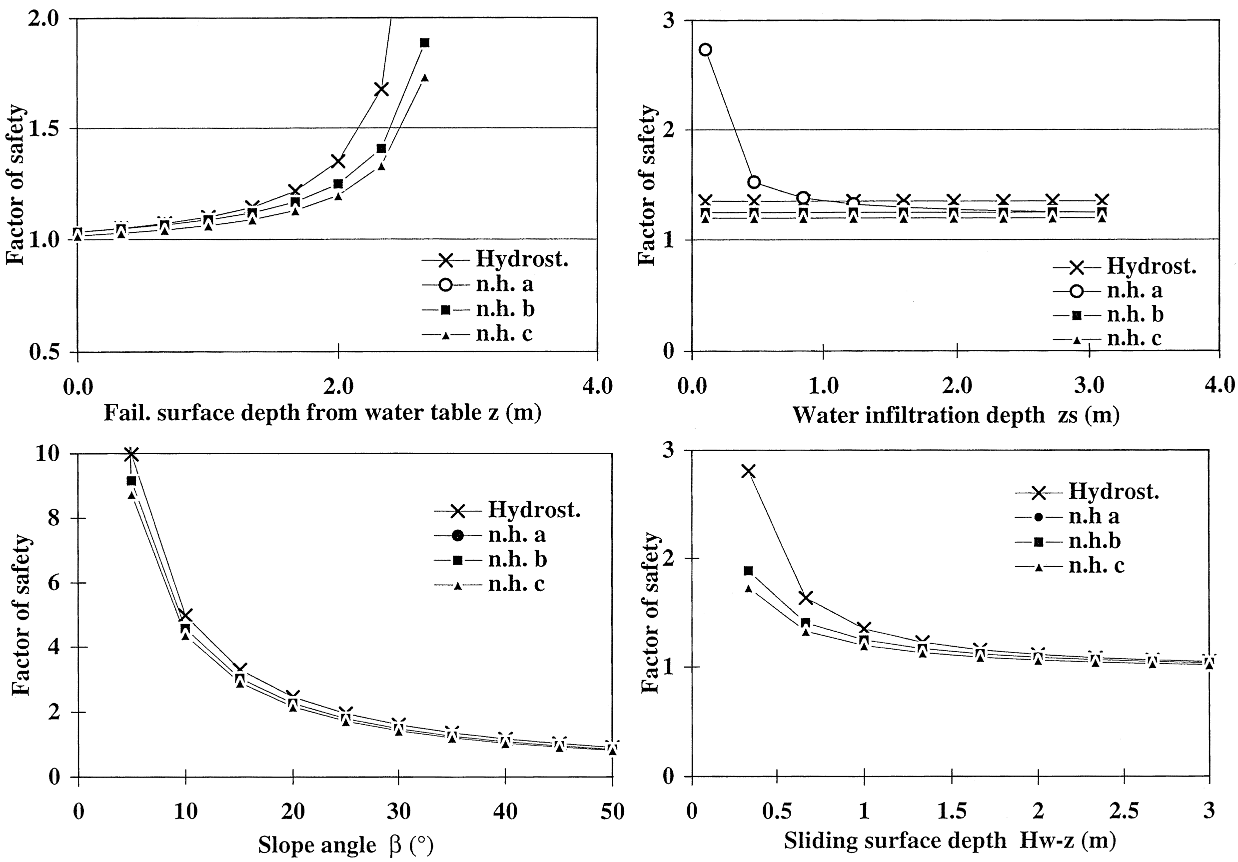

at which the rainfall intensity overcomes the soil saturated conductivity.
Seepage is a function of infiltration, soil properties, rainfall and local settings. Hydraulic characteristics and suction are the dominant soil properties, whereas rainfall intensity and duration are important rainfall characteristics leading to soil saturation. Other factors controlling the duration and quantity of the critical precipitation are soil moisture content and antecedent rainfall. The probability of reaching a critical saturation depth, and of initiating seepage, is controlled by all these factors, if water recharge from higher slope sectors and surficial runoff are neglected. The simultaneous failure of a large number of soil slips within a relatively large region, generally several tens of km^2, was recorded in different events at different sites (Valtellina 1987, Olona 1992, Varenna 1993, Langhe 1994). This coincidence can be interpreted as proof of the importance of regional or local thresholds, demonstrating the importance of specific rainfall, morphometric and soil characteristics.
Models based on soil characteristics were proposed to evaluate infiltration (Green and Ampt 1911; Lumb 1962). Pradel and Raad (1993) revised Green and Ampt's single-layer model, applying it to shallow slope stability problems. The model was partially modified introducing a better definition of warning and initiation thresholds. Four assumptions are made, namely: 1) soil surface is maintained constantly wet by water ponding; 2) a sharp wetted front exists; 3) the hydraulic conductivity is constant through the soil; and 4) the soil matrix suction at the front remains constant. Green and Ampt (1911) defined a 'characteristic time', i.e., a minimum rainfall intensity and a minimum permeability for vertical infiltration (Table 2) under the assumption that the rate of infiltration is less than or equal to the minimum rainfall intensity to allow for saturation (Wallace 1977; Kovacs 1981; Pradel and Raad 1993) and to allow for ponding. Ponding time (*Tp*) is the time elapsed between the beginning of rainfall and when water begins to pond on the soil surface. When ponding time is exceeded, the saturated zone extends deeper into the soil up to a 'critical infiltration depth'.
The relationships existing among rainfall intensity and duration, and soil properties including thickness and permeability, allow for rainfall and permeability thresholds to be identified different from those proposed by Pradel and Raad (1993), Crosta and Marchetti (1993) and Crosta (1994). The proposed model allowed the determination of the minimum rainfall intensity/duration values capable of yielding infiltration and saturation of the soil cover up to a critical depth after ponding (Fig. 10). Critical depth is either that previously assessed by slope stability analyses and field surveys or it can be estimated as the maximum saturable depth for a given rainfall. Pradel and Raad (1993) suggested that the intersection between thickness curves and intensity/duration curves plotted in the chart points out the intensity and duration minima needed for saturation of soils with a particular permeability and thickness. Adding curves obtained for constant hydraulic conductivity values (Crosta 1994), it was possible to separate different clusters, representing soils with different thickness and hydraulic properties. Any point above and to the right of this intersection represents intensity-duration conditions capable of saturating soil and producing seepage parallel to the slope.
Additionally, in the present work, with respect to the previous ones (Pradel and Raad 1993; Crosta and Marchetti 1993, Crosta 1994) we considered the ponding time. In fact, the introduction of ponding in the calculations induces a change in the pattern of thickness curves because of the "lag time" caused in starting the saturation. The delay is an inverse function of rainfall intensity and is asymptotic for low values of rainfall intensity comparable to low soil hydraulic conductivity. Runoff, evapotranspiration, and the effects of local groundwater recharge are not considered. Indeed, evapotranspiration can be neglected for relatively high-intensity phenomena. Evapotranspiration is important only during the first rainstorm of the season, or during episodic storms in the dry season. Any rainstorm with intensity (Eq. 12 in Table 2)

Table 2
Ponding and infiltration relationships obtained by Green and Ampt's (1911) model (Subscript *res* states that the parameters are considered during resaturation conditions; *k* hydraulic conductivity; *P* matric suction; n_{sat} wettable porosity; z_s depth of the wetting front)

Parameter	Equation	
Ponding time	$T_p = \dfrac{k_{res} P_{res} n_{sat}}{I(I - k_{res})}$	(9)
Characteristic time	$T_w = \dfrac{n_{sat}}{k_{res}}\left[z_s - P_{res} \ln\left(\dfrac{z_s + P_{res}}{P_{res}}\right)\right] + T_p$	(10)
Infiltration rate	$v_{\inf} = k_{res} \ln\left(\dfrac{z_s + P_{res}}{z_s}\right)$	(11)
Minimum rainfall intensity	$I_{\min} = \dfrac{n_{sat}}{T_{\min}}\left[z_s - P_{res} \ln\left(\dfrac{z_s + P_{res}}{P_{res}}\right)\right]\left(\dfrac{z_s + P_{res}}{z_s}\right)$	(12)
Permeability	$k_{\min} = \dfrac{n_{sat}}{T_{\min}}\left[z_s - P_{res} \ln\left(\dfrac{z_s + P_{res}}{P_{res}}\right)\right] = I_{\min}\left(\dfrac{z_s}{z_s + P_{res}}\right)$	(13)

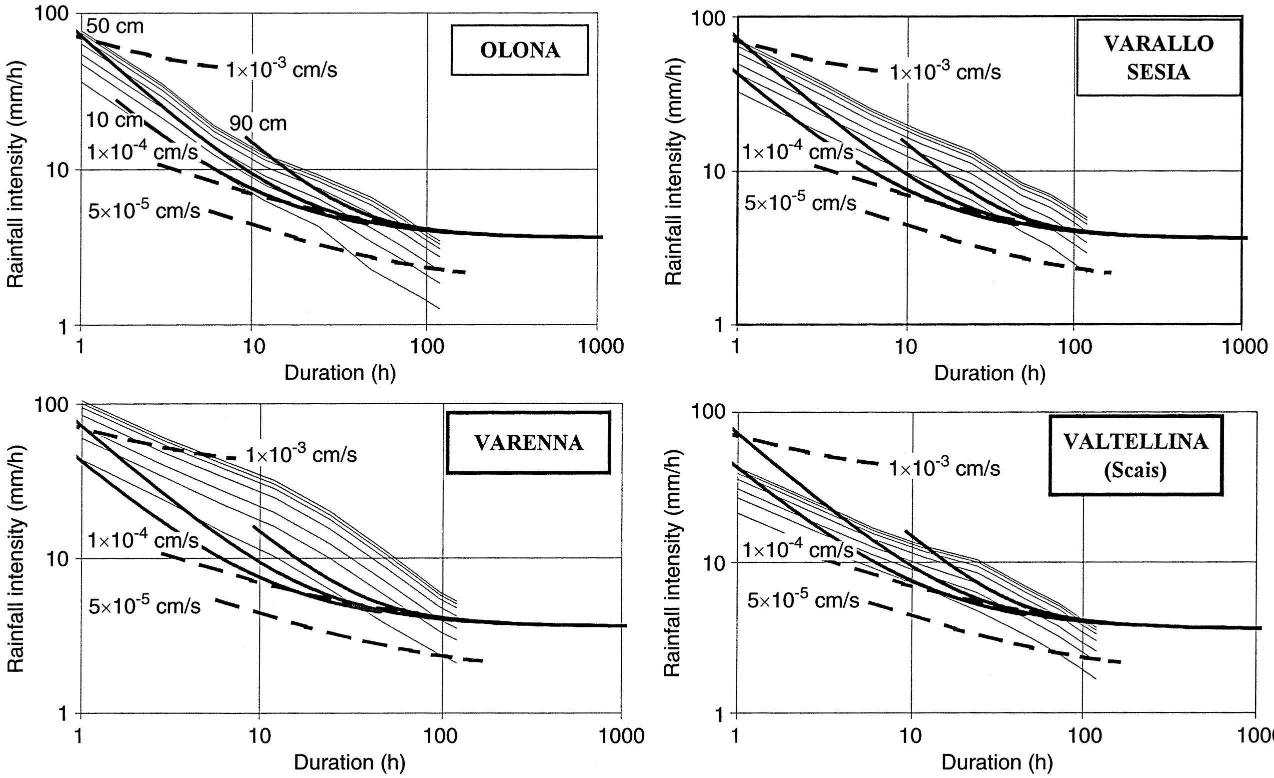

Fig. 10
Rainfall intensity vs duration plot for different recurrence time intervals (*thin lines* 2, 5, 10, 25, 50, 75, and 100 years moving upward). Three different permeability thresholds (*dashed thick lines*), typical of the soils studied, with three soil thickness curves (*thick continuous lines* 10, 50, and 90 cm) are traced on each plot. The asymptotic trend of the thickness curves is due to the introduction of ponding time (Tp, with $P_{suction} = 20$ cm)

and/or duration (Eq. 10 in Table 2) higher that the minimum value will cause saturation of a soil with given permeability, suction, wettable porosity and depth values. Pradel and Raad (1993) pointed out that soil with a permeability greater than a limiting value ("permeability threshold"; Eq. 13 in Table 2), will not saturate even if heavier rainfall with longer recurrence time intervals occur, because of the difficulty in reaching ponding conditions (Eq. 9 in Table 2). The proposed method for the initial definition of rainfall thresholds allows for the introduction of local characteristics (soil properties, rainfall characteristics, antecedent rainfall, morphometry, and ponding time) cutting out rainfall of lower intensity and long duration.

From hydrological modelling to slope stability analysis

When the hydrological model linking rainfall and infiltration had been defined, stability analyses could be performed, taking into consideration the pore-pressure distribution within the soil mass. Hydrostatic and nonhydrostatic conditions (Rahardjo and others 1995) represent different, or successive, phases of advancement of a wetting front. The hydrostatic condition reflects a dry period with no surficial saturation. Nonhydrostatic conditions characterize a slope where soil moisture changes due to a rainfall event. Going from a nonhydrostatic condition of a saturated surface (condition a, Eq. 6, Fig. 8) to that of a perched water table (condition c, Eq. 8, Fig. 8), a slope developes from pre-ponding conditions though the advancement of a wetting front to establishment of a perched water table.
It is interesting to plot the depth of the wetting front as a function of the time elapsed after ponding, together with the factor of safety for different conditions versus infiltration depth (z_s) and under the assumption that the most critical conditions occur for the coincidence of the failure surface and wetting front (Fig. 11). Safer conditions occur where the surface is saturated (type a). Slope instability increases going towards a pore-pressure distribution of type b and reach the minimum in the case of seepage parallel to the slope, with no suction contribution along the failure surface. This case was considered by Pradel and Raad (1993). Before a slope can fail due to a pore-pressure condition of type a, a lower factor of safety will be reached by advancement of the wetting front or the establishment of a perched water table.

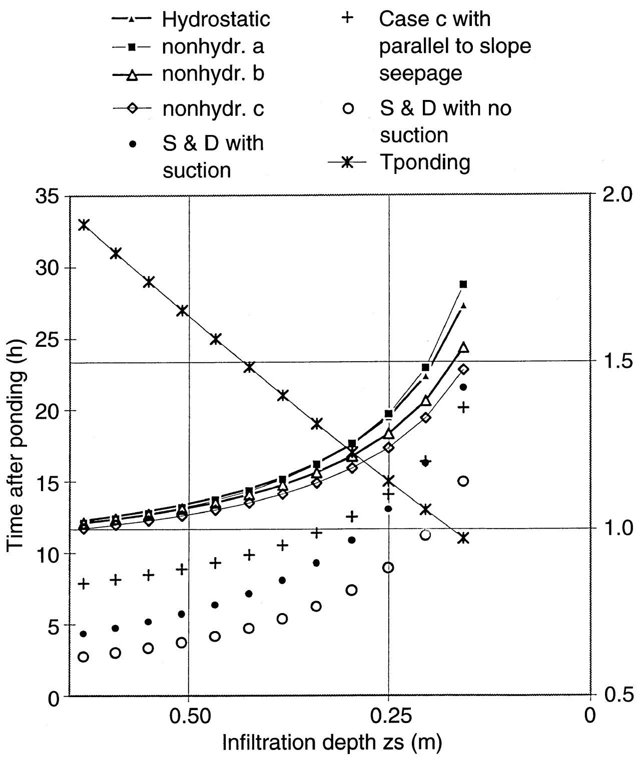

Fig. 11
Results of stability analyses by application of different approaches and conditions, summarized as factor of safety vs infiltration depth (*S & DL* Skempton and DeLory 1957; *n.h.* non-hydrostatic conditions). Time after ponding is also represented and can be used for a more precise definition of warning thresholds and to give a general idea of temporal changes in the factor of safety of the slope during a storm as a consequence of the deepening of the wetting front

Regionalization of rainfall thresholds

Rainfall thresholds are commonly defined as the line fitting the minimum intensity of rainfall associated with the occurrence of landslides in different areas (Caine 1980; Moser and Hohensinn 1983; Cancelli and Nova 1985, Wieczorek 1987). Local soil properties and antecedent rainfall are not normally taken into consideration when defining rainfall thresholds. Very few, physically based rainfall thresholds have been proposed that link rainfall, as well other hydrological events, and the hydrologic response of soil and local slope instability conditions (Buchanan and Savigny 1990; Pradel and Raad 1993; Wilson and Wieczorek 1995). This is the aim of second generation thresholds capable of zoning a territory taking into account local soil characteristics and the actual rainfall typical because of the peculiar meteorologic conditions of a particular region.
Figure 12 shows the rainfall intensity versus duration data for several events at different sites. Maximum hourly intensities are also plotted. Clusters of events can be identified within distinct permeability intervals (compare with Fig. 9). Events occurring in the Alpine, pre-Alpine and piedmont areas as well as events with or without antecedent rainfalls can be separated. Results of the clustering of events and the hydrological model used to identify rainfall thresholds, can be compared with the empirical, lower-bound thresholds, proposed in the literature for similar areas (Caine 1980; Govi and Sorzana 1980; Moser and Hohensinn 1983; Cancelli and Nova 1985; Wieczorek 1987; Ceriani and others 1992). The comparison shows that specific rainfall characteristics are particular to each region. Events in the Alps fall within a large sector of the

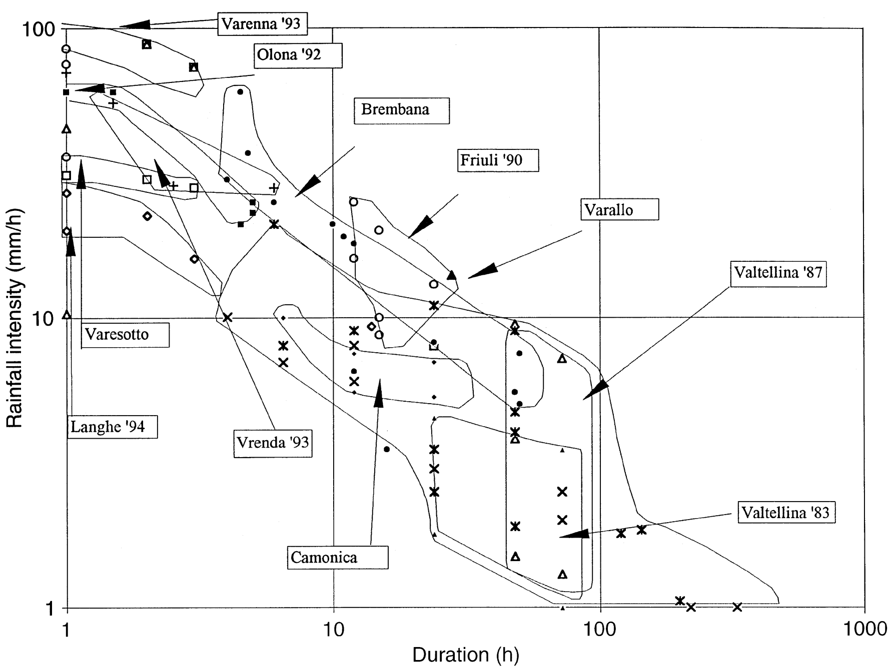

Fig. 12
Historical data for critical rainfall intensity and duration values related to soil slip occurrence collected from different sites. A simple subdivision of the plot is represented indicating regionalization of critical intensity/duration values

intensity-duration plot (Fig. 12). Data from Valtellina fall in a large section of medium- to low-intensity rainfall, with long to very long duration (Guzzetti and others 1992, Polloni and others 1992). The May 1983 and July 1987 events fall in the same area, with larger intensities recorded for the 1987 event. In Valtellina, the large scatter of data is due to the inclusion of events which occurred historically both on the southern (Orobic) and northern (Alpine) tributary valleys without differentiation. In fact, higher intensity rainfall regimes characterize the tributary valleys on the southern side from those lower intensity regimes on the northern side (Crosta 1990; Guzzetti and others 1992). Events occurring in the Camonica and Brembana Valleys in the pre-Alpine area fall into two sectors of the intensity-duration plot, reflecting a shorter duration and a higher intensity rainfall with respect to the Alpine events. The 1994 Valsesia failure is located in the middle part of the plot and exhibits high rainfall intensity. The 1992 and 1993 extreme events in the piedmont areas (Olona valley, Lake Maggiore) fall in the sector for highest intensity and lowest duration rainfall. A distinction can be made between the 1992 and 1993 events. The rainfall intensity that triggered shallow slope failures in the Olona Valley was higher than that recorded in the Varese and Lake Maggiore events. On the southern side of the Po Plain, in the Ligurian Alps, two situations can be recognized: maximum rainfall intensity for the 1993 event in the Varenna Valley; and a minimum rainfall intensity for the 1994 event in the Langhe region.

The data for hydraulic conductivity of soils and the failure thickness obtained from field surveys or back analyses (Fig. 10), could be overlained onto the same plot. This allows a better understanding of the events by separating permeability and thickness thresholds. These thresholds allow discrimination within the large range of soil types and thicknesses thereby identifying the storms that are of critical intensity and recurrence interval, given the prevailing ground conditions of a region. Observed and critical depths for the Valtellina events covered the low permeability field (1×10^{-5}–2×10^{-4} cm s^{-1}), with the 1983 event falling lower than the 1987 event. This is in agreement with descriptions reported in the literature (Cancelli and Nova 1985; Polloni and others 1992) and can be attributed to the high antecedent precipitation. High threshold permeabilities of 7×10^{-5}–1×10^{-3} cm s^{-1} can be associated with the Camonica and Brembana events. This geographical subdivision fits with what is proposed by Moser and Hohensinn (1983). Additionally, it justifies their classification by using physically based principles and takes into account the extreme rainfall conditions typical of each region.

Conclusions

Soil slips and debris flows are common evidence of extreme rainfall events in areas where terrain gradient and soil cover are favorable to slope instability. Many different rainfall thresholds have been proposed for the occurrence of soil slip and soil slip/debris flows, but few thresholds take into account local conditions. First generation rainfall thresholds as proposed by Caine (1980), Moser and Hohensinn (1983), Cancelli and Nova (1985), Wieczorek (1987) and Ceriani and others (1992) were mainly empirical. They were established by analyzing available data and defining lower bounds for the initiation of slope failures, without discerning among different soil properties or site specific rainfall conditions. More recently, second-generation warning thresholds were proposed by Keefer and others (1987), Buchanan and Savigny (1990) and Wilson and Wieczorek (1995) to overcome this limitation by using hydrological models. A future technical development with improved understanding of the rainfall/intensity relationship will be possible only on the basis of documented times of soil slip events (Keefer and others 1987).

Comparison of older and newer threshold models (Fig. 13) shows a certain similarity but suggests the imprecision of the first type. The application of a simple infiltration model (Green and Ampt 1911) to shallow slope failures (Pradel and Raad 1993) yields a promising approach to discriminate among critical and noncritical situations (Crosta and Marchetti 1993; Crosta 1994). While not lacking in limitations in the estimation of field values and their spatial variability, the approach includes some critical considerations, namely a better understanding of the influence of local factors such as morphology, geology, and geotechnical soil properties. Indeed, events from different locations have different characteristic features but, for each location, soil-slip thickness and time of failure differ only slightly. Only certain slopes, with particular soil types, can be saturated by specific rainfall events because of their physical properties.

Soils that can be saturated in southern Valtellina (Orobic side) by the typical regional rainfall are those with a threshold permeability close to 7×10^{-5} cm s^{-1}, while in northern Valtellina the limit is close to 2.5×10^{-4} cm s^{-1}. These threshold values were validated by means of in situ permeability tests, and remain valid for high recurrence time intervals (>50 year, Fig. 10). In the Olona Valley, both hydraulic conductivity and recurrence time interval are different (K>$8\times10^{-4h-}1\times10^{-3}$ cm s^{-1} for recurrence time >100 year). As a consequence, slopes in the Alpine regions (for example, Valtellina) are more subject to the mobilization of soils with medium and low permeabilities because of the site-specific rainfall conditions. Pre-Alpine areas (for example, the Camonica, Brembana and Sesia Valleys) exhibit higher susceptibility for soils with an intermediate range of permeabilities, while the piedmont area (Olona Valley, Varese and the Lake Maggiore) pertains to soils with higher permeability for landslide susceptible soils. These data, plotted on an intensity-duration diagram, are in agreement with the empirical subdivisions proposed by Moser and Hohensinn (1983).

The proposed model does not take into account the role of runoff and evapotranspiration. Rainfall required to

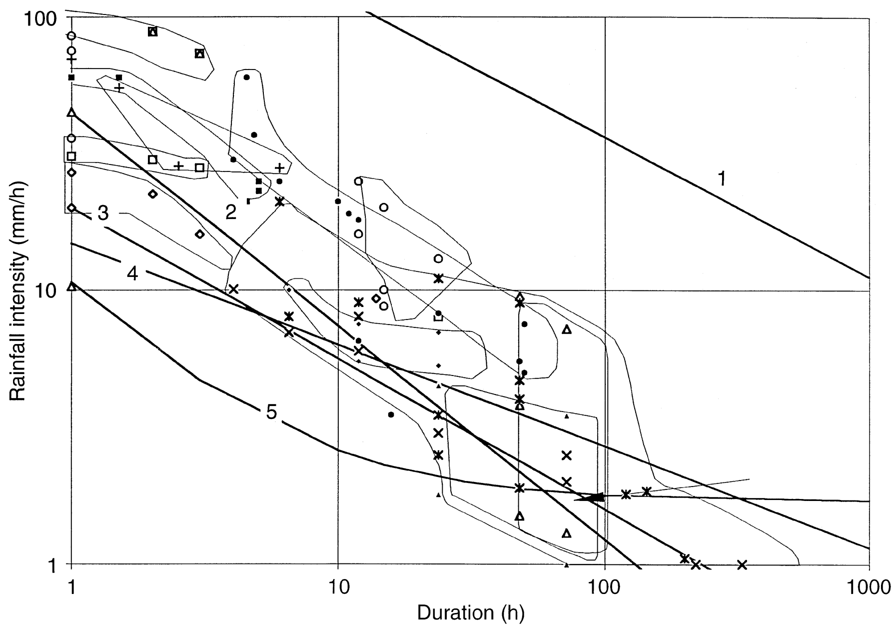

Fig. 13
Comparison of historical records, as subdivided in Fig. 12, with some empirical threshold relationships presented in the literature: *1* upper bound threshold, Caine 1980; *2* Cancelli and Nova 1985; *3* Ceriani and others 1992; *4* lower bound threshold, Caine 1980; *5* Wieczorek 1987

trigger shallow failures might be higher or longer than that computed. Recharge from uphill slope sectors and antecedent rainfall may play a considerable role in shifting threshold curves. As a result, if the change in moisture content is taken into account, all the events characterized by conspicuous antecedent rainfalls (for example, the 1983 Valtellina event) lie very close to the relative thickness curve (Fig. 10). By contrast, events characterized by limited antecedent rainfall (for example, Valtellina 1987, Olona 1992 and 1993, Langhe 1994) plot high with respect to their thickness curve, because of the effect of water runoff. This can be explained by the effect of antecedent rainfall on the wettable porosity. A decrease in the value of wettable porosity induces a leftward shift of the boundary lines, which counterbalances the effect of water losses for surficial runoff in the case of high intensity storms. A partial solution to this problem is suggested in this study by considering the effects of ponding time in delaying the advance of the wetting front. The effect is particularly evident for low-intensity and long-duration rainfall, characterized by long ponding times, and decreases for high-intensity and short-duration events, distinguished by very short ponding times.

The case of soil layers so thin as to become critical for instability must be emphasized. A thin soil cover will limit the number of failures in the absence of particular morphologic features and extremely unfavorable seepage flow directions. This is suggested by the average soil thickness of 0.3–0.6 m in association with shallow soil failures, with thicknesses close to or even below the lower limit only in the case of very steep (40°–45°) vegetated slopes, where soil slip/debris avalanches originated (Crosta 1990; Crosta and others 1990; Guzzetti and others 1992). A definition of the critical slope failure thickness is therefore important in defining shallow landslide susceptibility. The collection of field data and completion of stability analyses with different approaches and using probabilistic methods may prove an important aid to the assessment of hazards from shallow landslides.

Extreme rainfall conditions, when intensities remain high for long periods of time, must be accurately examined. In this case, any soil could become unstable. Hence, a better knowledge of the expected rainfall intensity and duration is fundamental for understanding the relationship with soil failure initiation and to establish different warning thresholds. Finally, the importance of a correct choice of models for performing slope stability analyses is stressed. Both the infiltration/saturation models and slope stability models to be used are, in fact, a function of the local characteristics and can vary through successive infiltration stages. Slopes with shallow bedrock become critical as a consequence of water flow at the bedrock-soil interface and of a rising water table. On the other hand, slopes with deep bedrock can suffer failures either due to water table rising or to a deepening wetting front.

Acknowledgements The author is deeply grateful to Fausto Guzzetti, Andy Hansen and Jerry Wieczorek for encouragement and for critical review of the paper.

References

Anderson SA, Sitar N (1995) Analysis of rainfall induced debris flows J Geotech Eng 121:544–552

Anselmo V (1980) Three case studies of storm and debris flows in north western Italy (Piemonte) In: Aulitzky A (ed) Proceedings of International Symposium Interpraevent 1980. Österr. Wasserwirtsch., Klagenfurt, pp 239–251

Baldi G, Beilin P, Brabb EE, Carrara A, Cardinali M, Cavallin A, Chiesa S, Crosta G, Detti R, Dovzak C, Floris B, Frassoni A, Guzzetti F, Marchetti M, Mark

R, Nozza G, Pasqui V, Reichenbach P (1990) Application of a geographic information system (GIS): landslide hazard maps. Memorie Società Geologica 45, pp 253–258
Buchanan P, Savigny KW (1990) Factors controlling debris avalanche initiation. Can Geotech J 27:659–675
Caine N (1980) The rainfall intensity duration control of shallow landslides and debris flows. Geogr Ann 62:23–27
Campbell RH (1974) Debris flows originating from soil slip during rainstorms in southern California. Q J Eng Geol London 7:339–349
Cancelli A, Nova R (1985) Landslides in soil debris cover triggered by rainstorms in Valtellina (central Alps, Italy) In: Sassa K (ed) Proceedings of 4th International Conference on Landslides, Tokyo, The Japanese Landslide Soc, Tokyo, pp 267–272
Casagrande A, Fadum RE (1940) Notes on soil testing for engineering purposes. Harvard University Soil Mechanics Series 8, Harvard University, Cambridge, Mass.
Ceriani M, Lauzi S, Padovan N (1992) Rainfalls and landslides in the Alpine area of Lombardia region, central Alps Italy. In: Aulitzky A (ed) Proceedings of Interpraevent 1992, Bern, Switzerland, Österr. Wasserwirtsch., Klagenfurt, 2:9–20
Costa JE, Wieczorek GF (eds) (1987) Debris flow/avalanches: process, recognition and mitigation. Reviews in Engineering Geology vol 7, Geological Society of America, Boulder, Colo.
Crosta G (1990) A study of slope movements caused by heavy rainfall in Valtellina (Italy – July 1987). In: Cancelli A (ed) Proceedings of ALPS90, Alpine Landslide Practical Seminar, 6th ICFL International Conference and Field Workshop on Landslides, Univ di Milano Spec Publ, Milan, Italy, pp 247–258
Crosta G (1994) Rainfall thresholds applied to soil slips in Alpine and pre-Alpine areas In: Proceedings 1st International Symposium on protection and development of the environment in mountain areas, Ponte di Legno, 20–24 June, Montana-Graf Galeati, pp 141–153
Crosta G, Marchetti M (1993) Frane superficiali nel medio tratto della Valle Olona. In: Del Prete M (ed) Proc. of 3rd Conv. Naz. Giov. Ricerc. Geol. Applicata, Potenza 28–30 October, Geol. Applicata e Idrogeologia, Bari, pp 327–337
Crosta G, Guzzetti F, Marchetti M, Reichenbach P (1990) Morphological classification of debris flow processes in south central Alps (Italy). In: Price DG (ed) Proceedings 6th International IAEG Congress, Balkema, Amsterdam, 3:1565–1572
Ellen S, Wieczorek GF (1988) Landslides, floods and marine effects of the storm of January 3–5 1982, in the San Francisco Bay Region, California. USGS Professional Paper 1434, U.S. Government Printing Office, Washington, DC
Govi M, Sorzana PF (1980) Landslide susceptibility as a function of critical rainfall amount in Piedmont basin (NW Italy). St Geomorph Carpatho-Balcanica, 14:43–61
Green WH, Ampt GA (1911) Studies on soil physics:1, flow of air and water through soils. J Agric Sci 4:1–24
Guzzetti F, Crosta G, Marchetti M, Reichenbach P (1992) Debris flows triggered by the 17–19 July, 1987 storm in the Valtellina area (Northern Italy). In: Aulitzky A (ed) Proceedings of Interpraevent 1992, Bern, Switzerland. Tagungspubl., Österr. Wasserwirtsch., Klagenfurt, 2:193–204
Iverson MR (1991) Sensitivity of stability analyses to groundwater data. In: Bell DH (ed) Proceedings of VIth International Symposium on Landslides, Christchurch, New Zealand. Balkema, Amsterdam, pp 451–457
Iverson MR, Major JJ (1986) Groundwater seepage vectors and the potential for hillslope failure and debris flow mobilization. Water Resour Res 22:1543–1548
Iverson MR, Reid ME (1992) Gravity driven groundwater flow and slope failure potential. 1. Elastic effective stress model. Water Resour Res 28:925–938
Keefer DK, Wilson RC, Mark RK, Brabb EE, Brown WM III, Ellen SD, Harp EL, Wieczorek GF, Alger CS, Zatkin RS (1987) Real-time landslide warning during heavy rainfall. Science 238:921–925
Kovacs G (1981) Seepage hydraulics. Elsevier, Amsterdam
Lumb P (1962) Effects of rainstorms on slope stability. In: Proceedings of the Symposium on Hong Kong Soils. GCO Publ., Hong Kong, pp 73–87
Moser M, Hohensinn F (1983) Geotechnical aspects of soil slips in Alpine regions. Eng Geol 19:185–211
Pierson TC (1983) Soil pipes and slope stability. Q J Eng Geol London 16:1–11
Pilgrim DH (1986) Bridging the gap between flood research and design practice. Water Resour Res 22:9, 165S–176S
Polloni G, Ceriani M, Lauzi S, Padovan N, Crosta G (1992) Rainfall and soil slipping events in Valtellina. In: Bell DH (ed) Proceedings of the VIth International Symposium on Landslides, Christchurch, New Zealand. Balkema, Amsterdam, pp 183–188
Polloni G, Aleotti P, Baldelli P, Nosetto A, Casavecchia K (1996) Heavy rain triggered landslides in the Alba area during November 1994 flooding event in the Piemonte region (Italy). In: Senneset K (ed) Proceedings of the VIIth International Symposium on Landslides, Trondheim, Norway. Balkema, Amsterdam, pp 1955–1960
Pradel D, Raad G (1993) Effect of permeability on surficial stability of homogeneous slopes. J Geotech Eng ASCE 119:315–332
Rahardjo H, Lim TT, Chang MF, Fredlund DG (1995) Shear strength characteristics of a residual soil. Can Geotech J 32:60–77
Reid MR, Iverson MR (1992) Gravity driven groundwater flow and slope failure potential. 1. Effects of slope morphology, material properties and hydraulic heterogeneity. Water Resour Res 28:939–950
Skempton AW, DeLory FA (1957) Stability of natural slopes in London Clay. In: Proceedings of the IVth International Conference ISSMFE (International Society for Soil Mechanics and Foundation Engineering), London, Butterworks 2:378–381
Wallace KB (1977) Moisture transients at the pavement edge: analytical studies of the influence of materials and cross section design. Geotechnique 27:497–516
Wieczorek GF (1987) Effect of rainfall intensity and duration on debris flows in central Santa Cruz Mountains, California. In: Costa JE, Weiczorek GF (eds) Debris flow/avalanches: process, recognition and mitigation. Reviews in Engineering Geology vol 7, Geological Society of America, Boulder, Colo., pp 93–104
Wilson RC, Wieczorek GF (1995) Rainfall thresholds for the initiation of debris flows at La Honda, California. Environ Eng Geosci 1:11–27